Haematologica
HAEMATOL/2021/278295
Version 4

Mechanical unloading aggravates bone destruction and tumor expansion in myeloma

Kotaro Tanimoto, Masahiro Hiasa, Hirofumi Tenshin, Jumpei Teramachi, Asuka Oda, Takeshi Harada, Yoshiki Higa, Kimiko Sogabe, Masahiro Oura, Ryohei Sumitani, Tomoyo Hara, Itsuro Endo, Eiji Tanaka, Toshio Matsumoto, and Masahiro Abe

Disclosures: M.A. received research funding from Chugai Pharmaceutical, Sanofi K.K., Pfizer Seiyaku K.K., Kyowa Hakko Kirin, MSD K.K., Astellas Pharma, Takeda Pharmaceutical, Teijin Pharma and Ono Pharmaceutical, and honoraria from Daiichi Sankyo Company. The other authors declare no competing financial interests.

Contributions: K.T., M.H. and M.A. designed the research and conceived the project. K.T., M.H., H.T., J.T., A.O., T.H., Y.H., K.S. M.O. and R.S. conducted animal experiments; T.H., I.E., T.M., E.T. evaluated muscle and bone specimens; K.T., M.H., K.S. M.O. and R.S. conducted in vitro cultures; K.T., M.H. J.T., H.T., A.O. T.H. and Y.H performed immunoblotting and immunohistochemical analyses; K.T., M.H. and A.O. performed flow cytometric analysis; and K.T., M.H. J.T. and H.T. performed transfection and PCR. K.T., M.H., I.E., T.M., E.T. and M.A. analyzed the data. K.T., M.H. and M.A. wrote the manuscript.

Title: Mechanical unloading aggravates bone destruction and tumor expansion in myeloma

Authors: Kotaro Tanimoto[1], Masahiro Hiasa[1], Hirofumi Tenshin[1], Jumpei Teramachi[2], Asuka Oda[3], Takeshi Harada[3], Yoshiki Higa[1] Kimiko Sogabe[3], Masahiro Oura[3], Ryohei Sumitani[3], Tomoyo Hara[3], Itsuro Endo[4], Toshio Matsumoto[5], Eiji Tanaka[1], and Masahiro Abe[3].

Affiliations: [1] Department of Orthodontics and Dentofacial Orthopedics, Tokushima University Graduate School of Biomedical Sciences, Tokushima, Japan; [2] Department of Oral Function and Anatomy, Okayama University Graduate School of Medicine, Dentistry and Pharmaceutical Science, Okayama, Japan; [3] Department of Hematology, Endocrinology and Metabolism, Tokushima University Graduate School of Biomedical Sciences, Tokushima, Japan; [4] Department of Bioregulatory Sciences, Tokushima University Graduate School of Medical Sciences, Tokushima, Japan. [5] Fujii Memorial Institute of Medical Sciences, Tokushima University, Tokushima, Japan

Corresponding authors: Masahiro Abe, Department of Hematology, Endocrinology and Metabolism, Tokushima University Graduate School, 3-18-15 Kuramoto, Tokushima, 770-8503, Japan, TEL: +81-88-633-7120, FAX: +81-88-633-7121, e-mail: masabe@tokushima-u.ac.jp; Masahiro Hiasa, Department of Orthodontics and Dentofacial Orthopedics, Tokushima University Graduate School of Biomedical Sciences, 3-18-15 Kuramoto, Tokushima, 770-8504, Japan, TEL: +81-88-633-7357, FAX: +81-88-633-9125, e-mail: mhiasa@tokushima-u.ac.jp

Acknowledgements: This work was supported in part by the JSPS KAKENHI Grant Numbers JP16K11504, JP17H05104, JP17KK0169, JP18K16118, JP18K08329, JP18H06294, JP19K21382 and 19K22719; and the Research Clusters program of Tokushima University. The funders had no role in study design, data collection and analysis, decision to publish, or preparation of the manuscript.

Competing Interests: M.A. received research funding from Chugai Pharmaceutical, Sanofi K.K., Pfizer Seiyaku K.K., Kyowa Hakko Kirin, MSD K.K., Astellas Pharma, Takeda Pharmaceutical, Teijin Pharma and Ono Pharmaceutical, and honoraria from Daiichi Sankyo Company. Other authors declare no competing financial interests.

Author Contributions: K.T., M.H. and M.A. designed the research and conceived the project. K.T., M.H., H.T., J.T., A.O., T.H., Y.H., K.S. M.O. and R.S. conducted animal experiments; T.H., I.E., T.M., E.T. evaluated muscle and bone specimens; K.T., M.H., K.S. M.O. and R.S. conducted *in vitro* cultures; K.T., M.H. J.T., H.T., A.O. T.H. and Y.H performed immunoblotting and immunohistochemical analyses; K.T., M.H. and A.O. performed flow cytometric analysis; and K.T., M.H. J.T. and H.T. performed transfection and PCR. K.T., M.H., I.E., T.M., E.T. and M.A. analyzed the data. K.T., M.H. and M.A. wrote the manuscript.

Word count: 1722 words, Figure count: 3 Figures and 3 Supplementary Figures

The importance of retaining physical functions has been increasingly emphasized to keep quality of life in patients with a variety of cancers, especially those with bone metastasis. Moreover, physical functions may impact prognosis of patients with cancers. Multiple myeloma (MM) has a unique propensity to develop and expand almost exclusively in the bone marrow and generate destructive bone disease. Patients with MM in advanced stages are often suffered from immobilization or a bed-ridden state with vertebral fracture and/or lower limb paralysis by spinal cord compression by tumors expanding outside of bone.

The skeleton and skeletal muscles are sensitive to their mechanical environment such as mechanical loading with exercise. Patients in a bed-ridden state or those with lower limb paralysis are exposed to mechanical unloading to decrease bone volume and strength along with muscle atrophy. However, the effect of mechanical unloading on the progression of MM tumor has not been studied. We hypothesized that immobilization or paralytic state not only negatively affects bone health but also may aggravate tumor growth in patients with MM. In the present study, we therefore aimed to clarify the deleterious impact of paralytic immobilization and mechanical unloading on tumor expansion and bone destruction in MM.

Unilateral hind legs of mice were immobilized to expose to mechanical unloading by sciatic denervation [1] or casting with adhesive bandage [2]. These procedures reduced hind leg muscle volume as shown by the weight as well as outer appearance of anterior tibial and gastrocnemius muscles at 2 weeks (Supplementary Figure 1A, B). Atrophy was more marked in the muscles in the hind legs paralyzed with sciatic denervation than those immobilized by casting with adhesive bandage. μCT revealed substantial reduction of bone volume in trabecular bone in the tibiae in the immobilized hind legs (Figure 1A). Bone morphometric analysis also showed reduction of bone volume in the immobilized hind legs, as indicated by increase of bone volume over total volume and trabecular numbers with reduced trabecular separation (Figure 1B). These μCT findings were consistent with the previous results in mice upon mechanical unloading with hind legs paralyzed by surgical denervation [1] and tail suspension [3]. Tartrate-resistant acid phosphatase (TRAP)-positive multinucleated osteoclasts increased in number on the surface of the trabecular bone in the immobilized hind legs (Figure 1C, D). TRAP-5b, a bone resorption marker, was increased in sera from the mice with hind legs paralyzed by sciatic denervation, while the levels of bone formation markers, bone alkaline phosphatase and osteocalcin, were not significantly changed in their sera (Figure 1E). These results demonstrate acute activation of bone

resorption by osteoclasts and thereby trabecular bone reduction alone with muscle atrophy in immobilized hind legs.

Osteocytes are embedded in the bone matrix, and major sensors of mechanical stress to regulate bone remodeling through interaction with bone marrow cells by their dendritic processes [4]. Osteocytes produce critical molecules for bone metabolism, including receptor activator of nuclear factor-κB ligand (RANKL) and its inhibitor osteoprotegerin (OPG), and sclerostin (SOST). After flushing out bone cavities to remove bone marrow cells, femurs were used for gene analysis in osteocytes embedded in bone. Consistent with the previous report [1], the gene expression of *Rankl* but neither *Opg* nor *Sost* was upregulated in the femurs from the hind legs immobilized with the sciatic denervation or casting (Figure 1F). Serum levels of Rankl were significantly increased in the mechanical unloading with sciatic denervation (Figure 1F). These results suggest that the role of RANKL upregulated in osteocytes in osteoclastogenesis enhanced in the immobilized hind legs.

We next looked at the effects of the immobilization or mechanical unloading of hind legs on MM tumor growth in bone. We inoculated luciferase-transfected mouse 5TGM1 MM cells into tibiae 2 weeks after sciatic denervation or sham operation, and compared tumor growth in hind legs with or without mechanical loading. Tumor growth was more robust in the immobilized hind legs with the denervation than in sham-operated hind legs as shown in IVIS images (Figure 1G). The previous reports demonstrated that osteoclasts directly enhance MM cell proliferation [5] and that RANKL-stimulated osteoclastogenesis triggers the proliferation of MM cells *in vivo* [6]. Indeed, osteoclasts generated from mouse bone marrow cells directly enhanced the growth of 5TGM1 cells (Supplementary Figure 2A). Because immobilization of legs acutely enhanced osteoclastogenesis (Figure 1C, D), osteoclasts induced in bone is suggested to play a causative role in MM cell expansion accelerated in mechanical unloading. Therefore, we next looked at the effects of the anti-bone resorbing agent zoledronic acid on MM tumor growth under hind leg immobilization. Treatment with zoledronic acid twice weekly after sciatic denervation maintained bone volume (Figure 2A) along with reduction of osteoclast numbers (Figure 2B, C). The treatment with zoledronic acid retarded the MM tumor growth in the immobilized hind legs (Figure 2D), suggesting the role of osteoclasts in the acceleration of MM tumor growth by immobilized hind legs.

To further confirm the acceleration of tumor growth in immobilized hind legs, we next

simultaneously inoculated 5TGM1 MM cells into bilateral tibiae in immobilized (right) and intact (left) hind legs in the same mice, and compared tumor growth between the immobilized or intact hind legs. MM tumor growth was assessed with IVIS images, and more accelerated in the immobilized legs with sciatic denervation (Figure 3A, top) or in those in a cast (Supplementary Figure 2B). We reported that Proviral Integrations of Moloney virus 2 kinase (PIM2) is constitutively overexpressed and further upregulated in MM cells through the interaction with cellular components in MM bone marrow microenvironment, including OCs [7]. We subsequently reported that TGF-β-activated kinase-1 (TAK1) is also overexpressed and phosphorylated to transcriptionally induce PIM2 expression in MM cells and OCs [8]. Consistently, CD138-positive MM cells and cathepsin K-positive OCs expressed both PIM2 and phosphorylated TAK1 in the tibiae with 5TGM1 MM cell inoculation (Supplemental Figure 3A). The TAK1 inhibitor LL-Z1640-2 as well as PIM inhibitor SMI16a are able to efficaciously reduce MM growth and osteoclastic bone destruction in *in vivo* MM models with 5TGM1 MM cells [8, 9], suggesting the pivotal role of the TAK1-PIM2 pathway in MM cells in MM tumor growth and bone destruction. Interestingly, TAK1 phosphorylation and PIM2 protein levels are further upregulated in MM tumor lesions in immobilized hind legs by sciatic denervation compared to those in intact hind legs (Figure 3B). TGF-β is released from the bone matrices through enhanced bone resorption, and activated by an acid and matrix metalloproteinases secreted from OCs. Consistently, the phosphorylation of Smad2 was increased in MM tumor lesions in immobilized hind legs by sciatic denervation (Figure 3B), which may in part contribute to the further activation of TAK1 in MM lesions under mechanical unloading with enhanced osteoclastogenesis. Importantly, treatment with the TAK1 inhibitor LL-Z1640-2 as well as the PIM inhibitor SMI16a was able to efficaciously reduce MM growth enhancement in the immobilized hind legs (Figure 3A), suggesting the therapeutic efficacy of these inhibitors under mechanical unloading. We are currently studying the therapeutic efficacy of LL-Z1640-2 and SMI16a in combination with proteasome inhibitors to maximize their anabolic as well as antitumor effects against MM.

In addition, we noticed that multiple palpable solid tumorous lesions appeared in mice with sciatic denervation over time at around 4 weeks or later at sites distant from the tibiae where MM cells were inoculated. To better analyze the metastatic expansion of MM cells inoculated into the tibiae, we transfected 5TGM1 MM cells with either *Gfp* (green fluorescent protein: GFP) or *Rfp* (red fluorescent protein: RFP) gene. The *in vitro* proliferation of the *Gfp*- and *Rfp*-transfected MM cells was the same (Supplementary

Figure 2C). The *Gfp*- and *Rfp*-transfected cells were inoculated into tibiae in right hind legs with sciatic denervation and left sham-operated hind legs, respectively. Tumor lesions were detected at sites distant from the tibiae at 4 weeks in IVIS images (Figure 3C). Interestingly, all the tumorous lesions metastasized outside of the tibiae were found to be composed of the MM cells labeled with GFP, indicating preferential extraosseous expansion of MM cells inoculated into tibiae in hind legs paralyzed with sciatic denervation. Furthermore, substantial numbers of GFP-positive cells but not RFP-positive cells were detected in sera drown from the mice at 4 weeks (Figure 3D). These results demonstrate the acceleration of MM tumor growth with egression from the bone marrow into circulation and thereby extraosseous dissemination under immobilization or mechanical unloading.

There were no significant changes in the serum levels of sclerostin (Supplementary Figure 3B) as well as *Sost* gene expression in mice with the sciatic denervation (Figure 1F). Robling et al. investigated the mechanoregulation of *Sost* mRNA and sclerostin under enhanced (ulnar loading) and reduced (hindlimb unloading) loading conditions [10]. *Sost* transcripts and sclerostin protein levels were significantly reduced at 24 hours in the ulna fixed to the loading platens and actuator after 360 cycles of mechanical loading per day. In contrast, mice subjected to tail suspension (hindlimb unloading) for 3 days exhibited a significant increase in *Sost* mRNA expression in the tibia compared to those in ground control mice. Intriguingly, this upregulation subsided to be non-significant after 7 days of the suspension. In our experiments, we analyzed *Sost* mRNA expression at 14 days after the immobilization, and found that *Sost* mRNA was not increased significantly. *Sost* mRNA induction by mechanical unloading may be temporal and should be studied in a time-sequence manner. However, serum levels of sclerostin has been demonstrated to be increased in MM patients with active bone lesions [11, 12] and positively correlate with lumbar spinal bone mineral density in postmenopausal women [13]. Consistent with the patients' observation, serum levels of sclerostin were increased after MM cell inoculation in mice, and more in mice with the mechanical unloading than in control mice (Supplementary Figure 3B), which may be due to the acceleration of MM tumor expansion by the mechanical unloading.

Bone is a unique microenvironment for MM cell growth and survival, providing niches to foster clonogenic and dormant MM cells. The present study demonstrates that hind leg immobilization or mechanical unloading aggravates bone destruction and MM tumor expansion. In contrast, mechanical loading with repeated forced compression [14] and low

intensity vibration [15] has been reported to suppress osteolysis and the growth of MM cells in bone. To keep bone mass in MM, repeated mechanical loading appears to play an important role. These observations warrant further study on the therapeutic merit of mechanical stress or loading in MM.

References

1. Miyazaki T, Zhao Z, Ichihara Y, et al. Mechanical regulation of bone homeostasis through p130Cas-mediated alleviation of NF-kappaB activity. Sci Adv. 2019;5(9):eaau7802.
2. Friedman MA, Zhang Y, Wayne JS, Farber CR, Donahue HJ. Single limb immobilization model for bone loss from unloading. J Biomech. 2019;83:181-189.
3. Amblard D, Lafage-Proust MH, Laib A, et al. Tail suspension induces bone loss in skeletally mature mice in the C57BL/6J strain but not in the C3H/HeJ strain. J Bone Miner Res. 2003;18(3):561-569.
4. Nakashima T, Hayashi M, Takayanagi H. New insights into osteoclastogenic signaling mechanisms. Trends Endocrinol Metab. 2012;23(11):582-590.
5. Abe M, Hiura K, Wilde J, et al. Osteoclasts enhance myeloma cell growth and survival via cell-cell contact: a vicious cycle between bone destruction and myeloma expansion. Blood. 2004;104(8):2484-2491.
6. Lawson MA, McDonald MM, Kovacic N, et al. Osteoclasts control reactivation of dormant myeloma cells by remodelling the endosteal niche. Nat Commun. 2015;6:8983.
7. Asano J, Nakano A, Oda A, et al. The serine/threonine kinase Pim-2 is a novel anti-apoptotic mediator in myeloma cells. Leukemia. 2011;25(7):1182-1188.
8. Teramachi J, Tenshin H, Hiasa M, et al. TAK1 is a pivotal therapeutic target for tumor progression and bone destruction in myeloma. Haematologica. 2021;106(5):1401-1413.
9. Hiasa M, Teramachi J, Oda A, et al. Pim-2 kinase is an important target of treatment for tumor progression and bone loss in myeloma. Leukemia. 2015;29(1):207-217.
10. Robling AG, Niziolek PJ, Baldridge LA, et al. Mechanical stimulation of bone in vivo reduces osteocyte expression of Sost/sclerostin. J Biol Chem. 2008;283(9):5866-5875.
11. Terpos E, Christoulas D, Katodritou E, et al. Elevated circulating sclerostin correlates with advanced disease features and abnormal bone remodeling in symptomatic myeloma: reduction post-bortezomib monotherapy. Int J Cancer. 2012;131(6):1466-1471.
12. Terpos E, Berenson J, Raje N, Roodman GD. Management of bone disease in

multiple myeloma. Expert Rev Hematol. 2014;7(1):113-125.

13. Polyzos SA, Anastasilakis AD, Bratengeier C, Woloszczuk W, Papatheodorou A, Terpos E. Serum sclerostin levels positively correlate with lumbar spinal bone mineral density in postmenopausal women--the six-month effect of risedronate and teriparatide. Osteoporos Int. 2012;23(3):1171-1176.

14. Rummler M, Ziouti F, Bouchard AL, et al. Mechanical loading prevents bone destruction and exerts anti-tumor effects in the MOPC315.BM.Luc model of myeloma bone disease. Acta Biomater. 2021;119:247-258.

15. Pagnotti GM, Chan ME, Adler BJ, et al. Low intensity vibration mitigates tumor progression and protects bone quantity and quality in a murine model of myeloma. Bone. 2016;90:69-79.

Figure legends.

Figure 1. Enhancement of osteoclastogenesis and MM tumor growth by immobilization.

SCID mice were subject to sham-operation (control), sciatic denervation (DN) or casting with adhesive bandages (CAST) in right hind legs. Two weeks later, the right tibiae were taken out, and histomorphometrically analyzed. (**A**) μCT image of the representative tibiae resected from each treatment group. (**B**) Tibiae were resected from mice, carefully separated from surrounding tissues, and fixed overnight in 10 % formaldehyde solution. The dissected tibiae were then examined with a SkyScan 1176 unit (SkyScan 1176 scanner and analytical software; Buruker, Billerica, MA) using a 0.5 mm aluminium filter, rotation of 360°, rotation step of 0.5°, voltage of 50 kV, current of 200 μA and image size of 18 μm voxel size. The regions of interest for trabecular bones analyzed with a μCT were set on a 1.5 mm region of metaphyseal spongiosa in the proximal tibia located 0.5 mm above the growth plate. The threshold was set with 93 (lower) and 255 (upper), which was able to clearly indicate the trabecular bone. Bone volume over total volume (BV/TV), trabecular thickness (Tb.Th), trabecular numbers (Tb.N) and trabecular separation (Tb.Sp) were assessed in trabecular bones. Data are expressed as the mean ± SD (n = 6). (**C**) TRAP staining was performed in the sections of the resected tibiae using a TRAP/ALP stain kit (FUJIFILM Wako Chemicals USA, Richmond, VA, USA). TRAP-positive cells containing 3 or more nuclei on the bone surface were counted as OCs under a light microscope (BZ-X800; Keyence, Osaka, Japan). Three fields were counted for each sample. Representative results were shown (magnification, ×100) (upper). Bars: 200 μm. Higher magnification (×400) of the boxed areas in the upper panels were shown in the lower panels. Bars: 50 μm. (**D**) Numbers of osteoclasts (N.Oc)/bone surface (BS) (/mm) were counted. Data are expressed as the mean ± SD (n = 6). *p < 0.05. (**E**) Serum levels of TRAP-5b (μg/mL), ALP (μU/mL) and Gla-osteocalcin (OCN) (ng/mL) were measured 2 weeks after the DN. To measure the serum levels of bone metabolic parameters, Mouse Osteocalcin EIA Kit (Biomedical Technologies Inc., MA, USA), Mouse TRAP-5b Assay (Immuno diagnostic system Ltd, UK), and alkaline phosphatase (ALP) test kit (Wako, Osaka, Japan) were used in accordance with the manufactures' protocols. Data are expressed as the mean ± SD (n = 6). *p < 0.05. (**F**) Femurs were taken out at 2 weeks after the immobilization, and their bone marrow cavities were flushed out. Expression of *RANKL*, *SOST*, and *OPG* mRNA were analyzed by real-time RT-PCR using the femurs. The primer sequences were as follows: mouse *Rankl* F: GTTCCTGTACTTTCGAGCGCAGAT, R:

TGACTTTATGGGAACCCGATGGGA mouse *Opg* F: TTGCCCTGACCACCACTCTTATACGGA, R: CTTTTGCGTGGCTTCTCTCTGTTTCC mouse *SOST* F: TCCTCCTGAGAACAACCAGAC, R: TGTCAGGAAGCGGGTAGTC mouse *Gapdh F*: ATGTGTCCGTCGTGGATCTGA, R: TTGAAGTCGCAGGAGACAACCT. Serum level of RANKL (pg/mL) were measured by Mouse TRANCE/RANKL/TNFSF11 ELISA kit (R&D systems). Data are expressed as the mean ± SD (n = 6). *p < 0.05. (**G**) Luciferase-transfected 5TGM1 (5TGM1/luc) MM cells were inoculated into tibiae 2 weeks after DN or sham operation. Two weeks after the immobilization, we injected $1x10^4$ 5TGM1/luc MM cells in 20 μL saline, and directly through the tibial plateau into the bone marrow cavity of the tibiae with a 27-gauge needle while flexing the knee. IVIS images were taken 2 and 4 weeks after the inoculation. Tumor areas with luminescence shown in green, yellow and red were measured. Px, pixel. Data are expressed as the mean ± SD (n =3). *p < 0.05.

Figure 2. Effects of zoledronic acid on MM tumor growth upon immobilization.

Mice were subjected to sham-operation (control), sciatic denervation (DN) or casting with adhesive bandages (CAST) in right hind legs. Zoledronic acid (ZOL, 120 μg/kg) or saline were subcutaneously injected twice a week. Two weeks later, the right tibiae were taken out, and histomorphometrically analyzed. (**A**) Bone volume over total volume (BV/TV), trabecular thickness (Tb.Th), trabecular numbers (Tb.N) and trabecular separation (Tb.Sp) were assessed in trabecular bones. Data are expressed as the mean ± SD (n = 6). (**B**) TRAP staining was performed in the resected tibiae. Representative results were shown (magnification, ×100) (upper). Bars: 200 μm. Higher magnification (×400) of the boxed areas in the upper panels were shown in the lower panels. Bars: 50 μm. (**C**) Numbers of osteoclasts (N.Oc)/bone surface (BS) (/mm) were counted. Data are expressed as the mean ± SD (n = 6). **p < 0.01. (**D**) Mice were subjected to sham-operation (control), sciatic denervation (DN) in right hind legs. 5TGM1/luc MM cells were inoculated into the right tibiae 2 weeks after DN or sham operation. The mice were subcutaneously injected with 120 μg/kg zoledronic acid (ZOL) or saline twice a week. IVIS images were taken 4 weeks after the inoculation. Control groups were given saline as a vehicle. For IVIS imaging, 100 μL of 15 mg/mL D-luciferin in PBS was injected i.p. to mice before taking images. Five minutes after D-luciferin injection, place the mice in the imager. The mice were anesthetized with 2% isoflurane while taking IVIS images. Tumor areas with luminescence shown in green, yellow and red were measured. Px, pixel. Data are expressed as the mean ± SD (n = 5). **p < 0.01.

Figure 3. MM tumor growth and dissemination upon immobilization.
(**A**) Right and left hind legs in the same mice were subjected to sciatic denervation and sham- operation, respectively. Two weeks later, luciferase-transfected mouse 5TGM1 MM cells were simultaneously inoculated into tibiae in both immobilized (right) and intact (left) hind legs in the same mice. The TAK1 inhibitor LL-Z1640-2 or the PIM inhibitor SMI16a were intraperitoneally injected at 20 mg/kg twice a week. Control groups were given saline as a vehicle. IVIS images taken at 3 weeks. Tumor areas with luminescence shown in green, yellow and red were measured. Px, pixel. Data are expressed as the mean ± SD (n = 5). **p < 0.01. (**B**) 5TGM1 MM cells were inoculated into right tibiae 2 weeks after sciatic denervation (DN) or sham operation. The right tibiae with tumor lesions were harvested at 4 weeks after the MM cell inoculation. Cell lysates were then collected from MM tumor lesions, and protein levels of the indicated factors were analyzed by Western blotting analysis. β-actin was used as a loading control. The following reagents were purchased from the indicated manufacturers: antibodies against phosphor-MAP3K7 (Thr187) from Cusabio (Cusabio Biotech, Wuhan, China); and antibodies against TAK1, PIM2, phosho-Smad2, Smad2, and β-actin from Cell Signaling Technology. (**C**) 5TGM1 MM cells transfected with *Gfp* (green fluorescent protein) or *Rfp* (red fluorescent protein) genes were inoculated into tibiae in right hind legs with sciatic denervation and left sham-operated hind legs, respectively. The GFP-expressing 5TGM1/luc (5TGM1-GFP/Luc) cell line and the RFP-expressing 5TGM1/luc (5TGM1-RFP/Luc) cell line were generated by lentiviral transduction with the pLKO.1-puro-CMV-TurboGFP vector and pLKO.1-puro-CMV-TagRFP vector (Sigma-Aldrich, MO, USA), respectively. Four weeks later, IVIS images were taken. Blood was drawn from retro-orbital plexus, and tumors detected in the IVIS images were resected with surrounding tissues in the mice. Tumors emitting green or red fluorescence were visualized in resected samples with a fluorescence microscope (OLYMPUS SZX16). (**D**) Circulating 5TGM1-GFP and 5TGM1-RFP cells were analyzed in the blood samples from the mice at 4 weeks by flow cytometer.

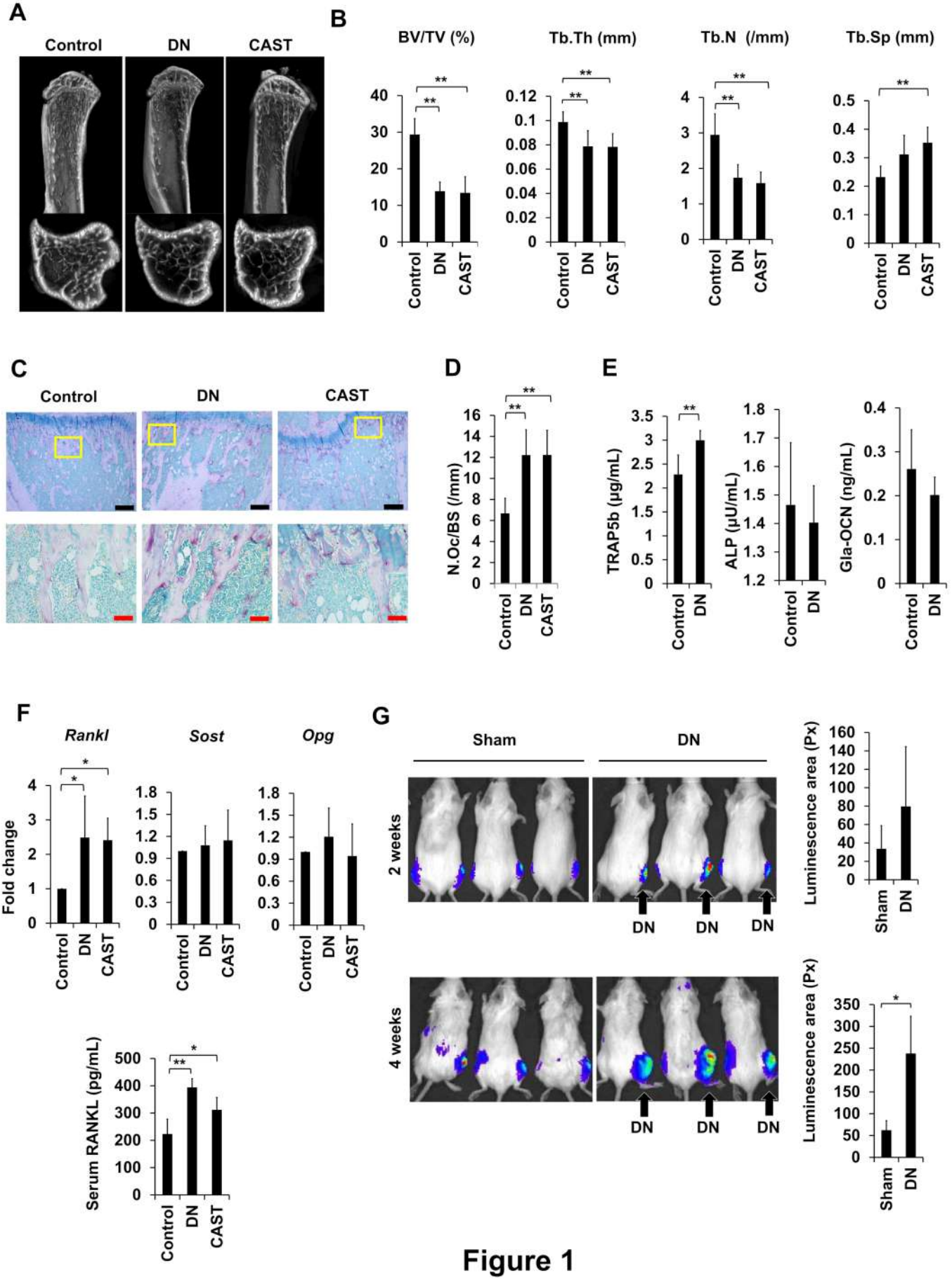
A
Control
DN
CAST
B
BV/TV (%)
Tb.Th (mm)
Tb.N (/mm)
Tb.Sp (mm)
Control
DN
CAST
C
Control
DN
CAST
D
N.Oc/BS (/mm)
E
TRAP5b (μg/mL)
ALP (μU/mL)
Gla-OCN (ng/mL)
F
Rankl
Sost
Opg
Fold change
Serum RANKL (pg/mL)
G
Sham
DN
2 weeks
4 weeks
Luminescence area (Px)

Figure 1

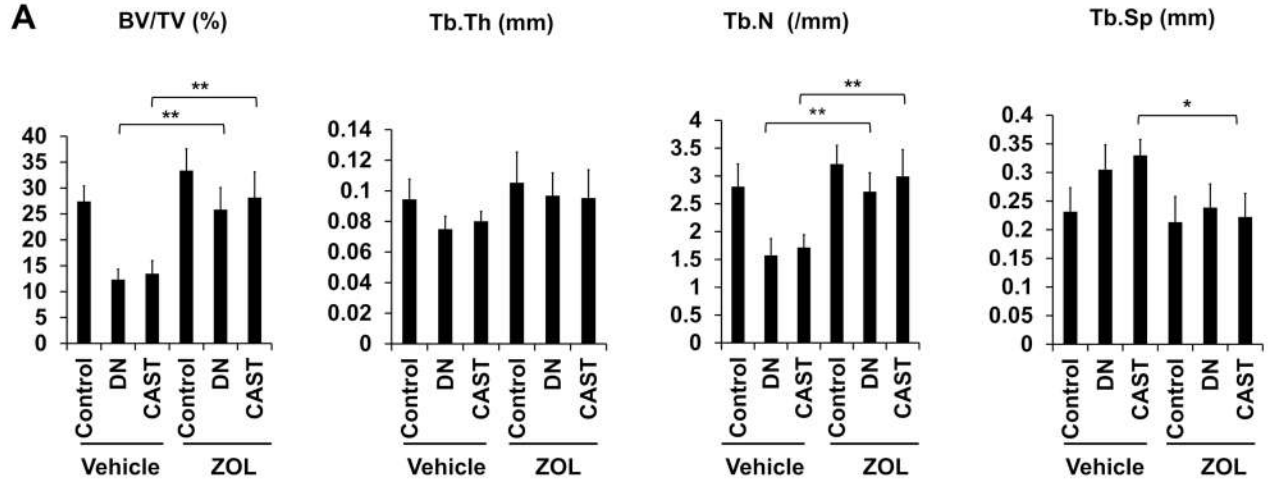
A
BV/TV (%)
Tb.Th (mm)
Tb.N (/mm)
Tb.Sp (mm)
Control
DN
CAST
Vehicle
ZOL

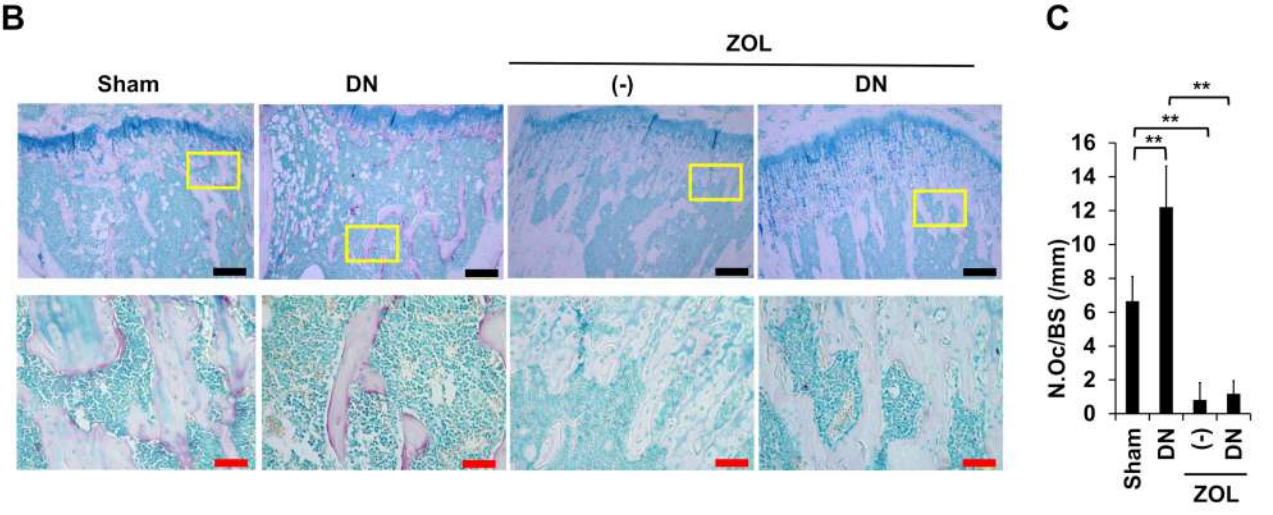
B
Sham
DN
ZOL
(-)
DN

C
N.Oc/BS (/mm)
Sham
DN
(-)
DN
ZOL

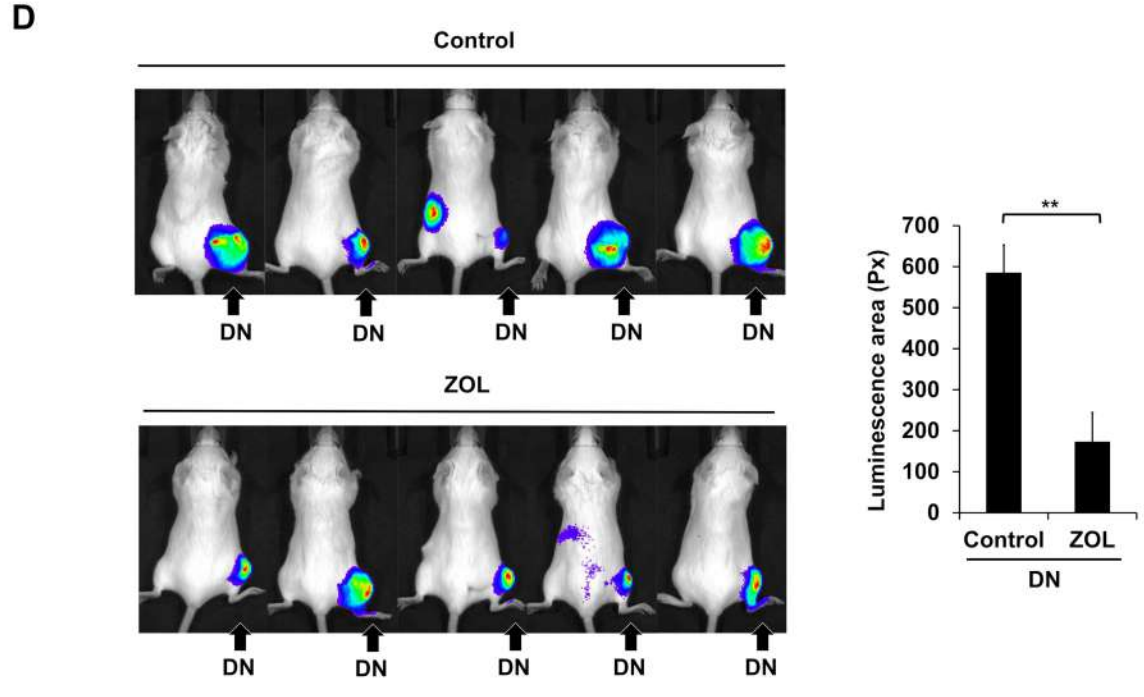
D
Control
DN
ZOL
Luminescence area (Px)
Control
ZOL
DN

Figure 2

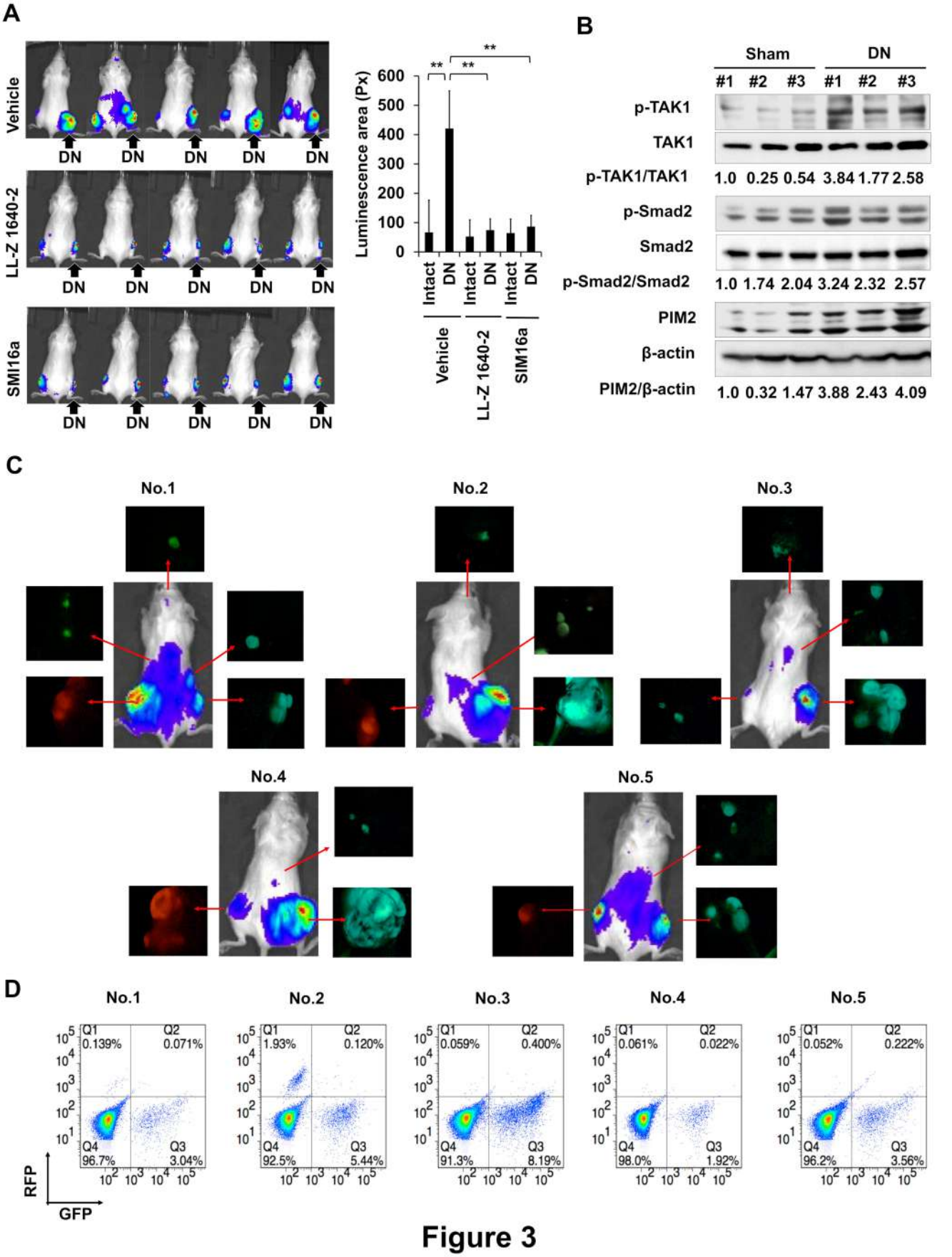
A
Vehicle
LL-Z 1640-2
SMI16a
DN
Luminescence area (Px)
600
500
400
300
200
100
0
**
**
**
Intact
DN
Vehicle
LL-Z 1640-2
SIM16a
B
Sham
DN
#1 #2 #3 #1 #2 #3
p-TAK1
TAK1
p-TAK1/TAK1
1.0 0.25 0.54 3.84 1.77 2.58
p-Smad2
Smad2
p-Smad2/Smad2
1.0 1.74 2.04 3.24 2.32 2.57
PIM2
β-actin
PIM2/β-actin
1.0 0.32 1.47 3.88 2.43 4.09
C
No.1
No.2
No.3
No.4
No.5
D
No.1
Q1 0.139%
Q2 0.071%
Q4 96.7%
Q3 3.04%
No.2
Q1 1.93%
Q2 0.120%
Q4 92.5%
Q3 5.44%
No.3
Q1 0.059%
Q2 0.400%
Q4 91.3%
Q3 8.19%
No.4
Q1 0.061%
Q2 0.022%
Q4 98.0%
Q3 1.92%
No.5
Q1 0.052%
Q2 0.222%
Q4 96.2%
Q3 3.56%
RFP
GFP

Figure 3

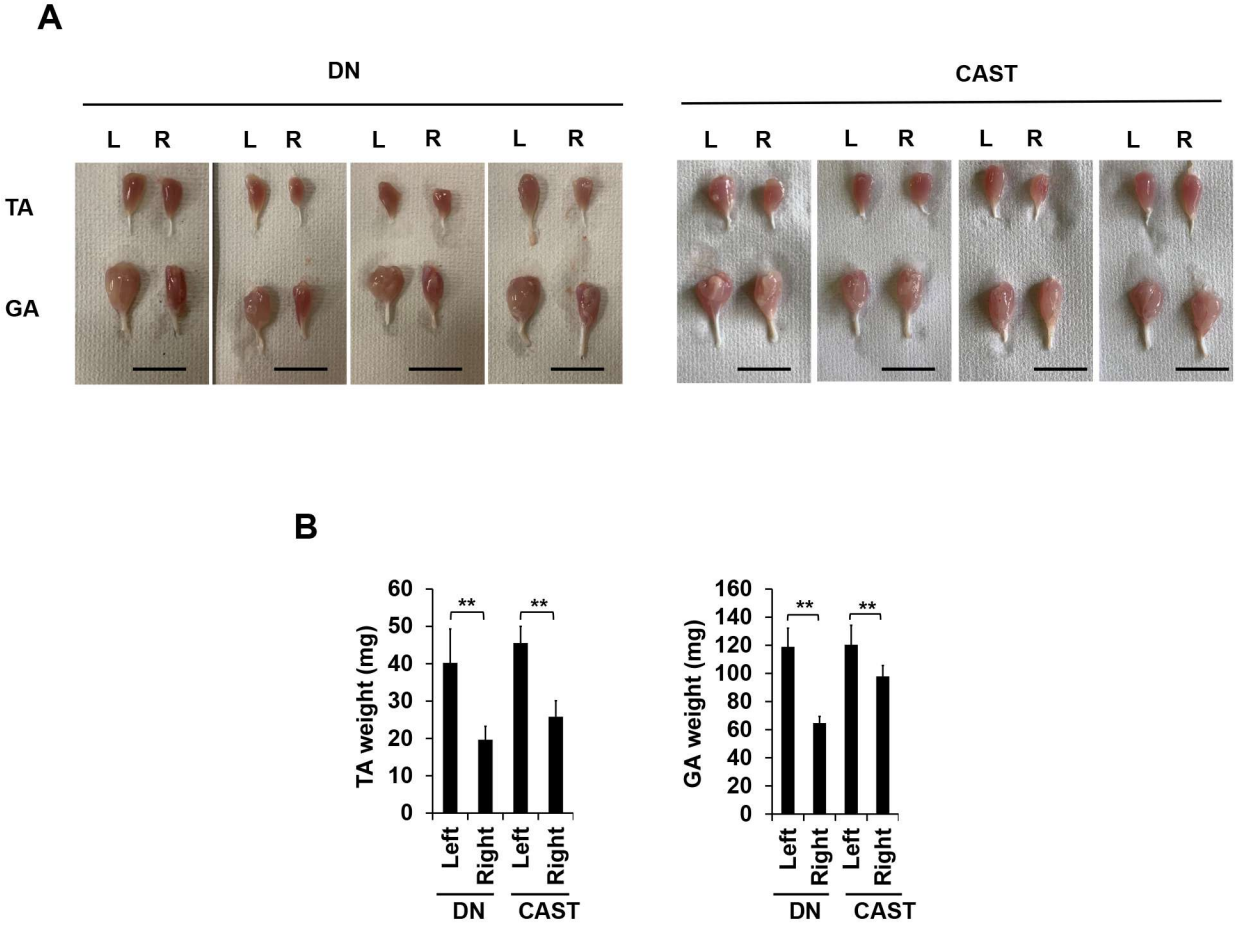

Supplementary Figure 1

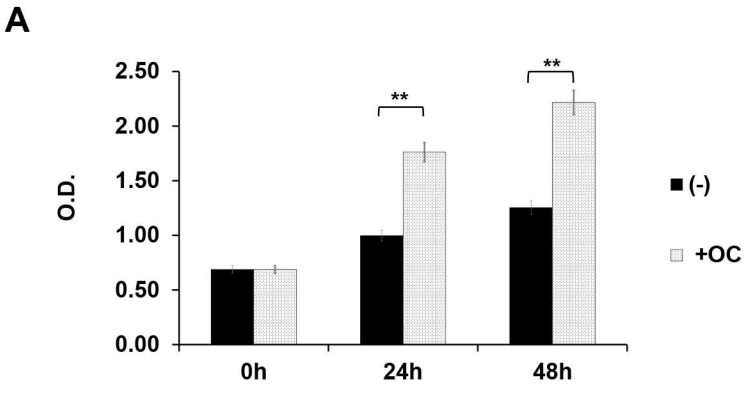

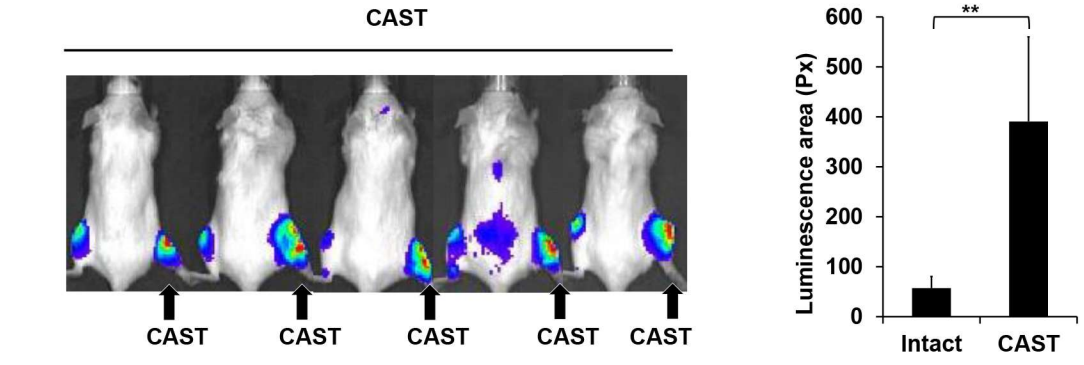

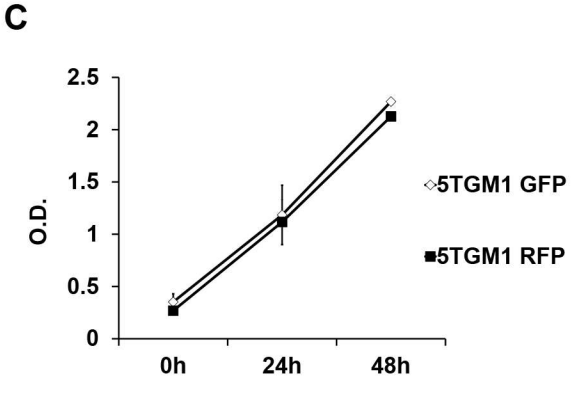

Supplementary Figure 2

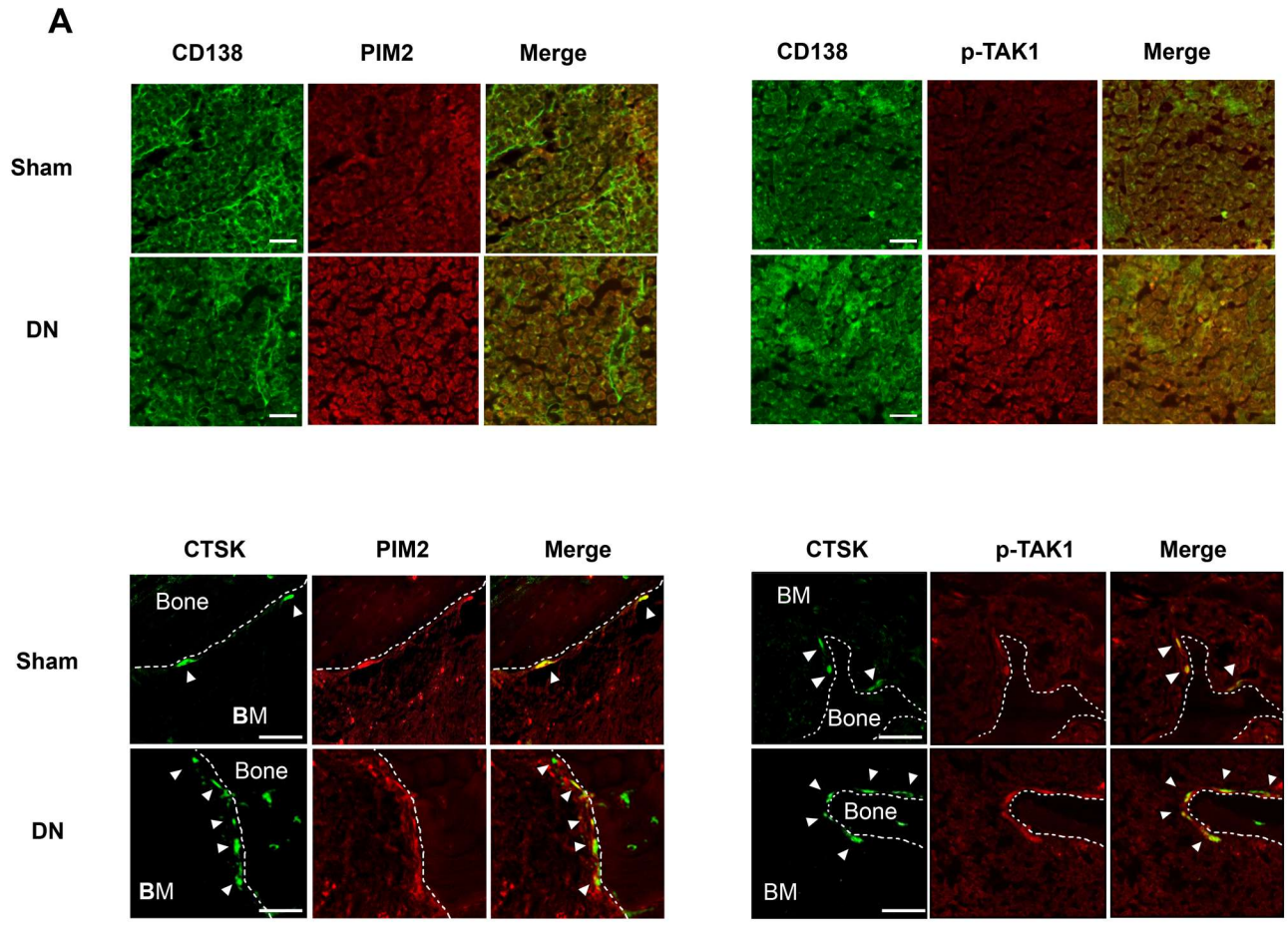

Supplementary Figure 3